Molecular dynamics of fully biobased poly(butylene 2,5-furanoate) as revealed by broadband dielectric spectroscopy

Accepted Manuscript

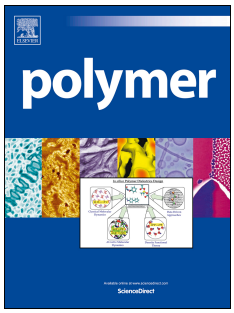

Molecular dynamics of fully biobased poly(butylene 2,5-furanoate) as revealed by broadband dielectric spectroscopy

Michelina Soccio, Daniel E. Martínez-Tong, Angel Alegría, Andrea Munari, Nadia Lotti

PII: S0032-3861(17)30869-8

DOI: 10.1016/j.polymer.2017.09.007

Reference: JPOL 19976

To appear in: *Polymer*

Received Date: 14 June 2017

Revised Date: 24 August 2017

Accepted Date: 3 September 2017

Please cite this article as: Soccio M, Martínez-Tong DE, Alegría A, Munari A, Lotti N, Molecular dynamics of fully biobased poly(butylene 2,5-furanoate) as revealed by broadband dielectric spectroscopy, *Polymer* (2017), doi: 10.1016/j.polymer.2017.09.007.

Graphical Abstract

Molecular dynamics of fully biobased poly(butylene 2,5-furanoate) as revealed by broadband dielectric spectroscopy

Michelina Soccio[a], Daniel E. Martínez-Tong[b,c], Angel Alegría[c,d], Andrea Munari[a], Nadia Lotti[a]

[a]Civil, Chemical, Environmental and Materials Engineering Dept., University of Bologna, Via Terracini 28, 40131, Bologna, Italy
[b]Donostia International Physics Center. P. Manuel Lardizabal 4. 20018, Donostia, Spain.
[c]Centro de Física de Materiales (CSIC-UPV/EHU). P. Manuel Lardizabal 5. 20018, Donostia, Spain.
[d]Departamento de Física de Materiales. Basque Country University (UPV/EHU). Apdo 1072. 20080, Donostia, Spain.

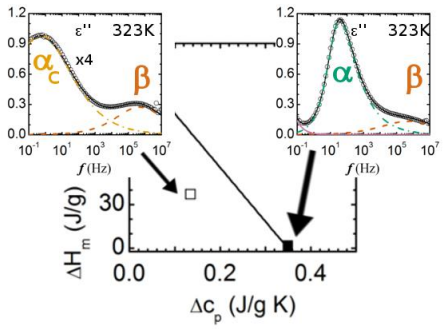

Molecular dynamics of fully biobased poly(butylene 2,5-furanoate) as revealed by broadband dielectric spectroscopy

Michelina Soccio[a,*], Daniel E. Martínez-Tong[b,c,*], Angel Alegría[c,d], Andrea Munari[a], Nadia Lotti[a]

[a]Civil, Chemical, Environmental and Materials Engineering Dept., University of Bologna, Via Terracini 28, 40131, Bologna, Italy
[b]Donostia International Physics Center. P. Manuel Lardizabal 4. 20018, Donostia, Spain.
[c]Centro de Física de Materiales (CSIC-UPV/EHU). P. Manuel Lardizabal 5. 20018, Donostia, Spain.
[d]Departamento de Física de Materiales. Basque Country University (UPV/EHU). Apdo 1072. 20080, Donostia, Spain.

*corresponding authors: m.soccio@unibo.it
danielenrique_martineztong001@ehu.eus

Abstract

This work presents the molecular dynamics of both fully amorphous and semicrystalline poly(butylene 2,5-furanoate) (PBF). Broadband dielectric spectroscopy experiments were combined with temperature modulated differential scanning calorimetry measurements. The results showed that the subglass molecular dynamics is characterized by the existence of two dielectric relaxation processes, being the faster one associated to the glycolic subunit, whereas the slower relaxation was assigned to the link in between the ester group and the furan ring. Crystallization affected differently the contribution of these two components. Additionally, crystallization had a stronger effect on the α relaxation process, related to the segmental dynamics of the amorphous phase. In the semicrystalline state, the PBF amorphous phase was described as being composed by different fractions, including a completely rigid one, with distinctly slower mobilities and reduced contributions to the dielectric relaxation, compared to the fully amorphous polymer.

Keywords: poly(butylene 2,5-furanoate), broadband dielectric spectroscopy, semicrystalline polymers, rigid amorphous fraction, molecular dynamics.

1. Introduction

The increasing awareness concerning the use of fossil fuels and human impact on the environment has led to a renewed strong interest in the use of sustainable resources for energy and materials.[1-3] Among the different renewable raw materials that have been used for the preparation of bioplastics, furan-based monomers have attracted considerable attention; the most important example being represented by 2,5-furandicarboxylic acid (2,5-FDCA). This monomer is mainly used for the synthesis of poly(ethylene-2,5-furanoate) (PEF), considered the most credible biobased alternative to poly(ethylene terephthalate) (PET).[1-5] In fact, PEF displays more attractive thermal and mechanical response and improved barrier properties than PET: higher glass transition temperature (T_g) (358 K *vs* 349 K) and lower melting temperature (T_m) (484 K *vs* 520 K),[4,5] a 1.6 times higher Young's modulus,[6] 11 times lower oxygen permeability,[7] 19 times lower carbon dioxide permeability[8] and a 5 times lower water diffusion coefficient.[9] Last but not least, the production of PEF would decrease the non-renewable energy use of about 40-50% and the greenhouse gas emissions of 45-55% ca. with respect to PET.[10] Furthermore, other 2,5-furan dicarboxylate-based polymers have been synthesized using aliphatic diols with different lengths, for example, sugar diols like isosorbide, benzylic structures like 1,4-bishydroxymethyl benzene, and bisphenols like hydroquinone.[6] In this framework, it has been recently reported the synthesis of the poly(butylene 2,5-furanoate) (PBF) and its copolymers: these reports showed that PBF had good thermal, mechanical[6,11-18] and barrier properties,[11] in line with those expected for possible industrial applications such as food packaging.

As reported in the literature[5,11,17] several of these furan-based polymers can crystallize under the appropriate conditions, leading to the development of a semicrystalline material, *i.e.* a polymer composed by phase-separated amorphous and crystalline areas. This fact is very interesting from the applications point of view since semicrystalline polymers have enhanced thermal and mechanical properties, and better chemical resistance. However, polymer crystallization is a complicated process that might significantly alter the properties of the remaining amorphous phase.[19] A powerful way of investigating the semicrystalline polymer amorphous phase is by probing its molecular dynamics; particularly, the segmental relaxation is directly connected with the characteristics of the glass transition process, and polymer crystals impose structural constrains affecting these segmental motions.[19-22] However, the details of these effects can be hardly anticipated. Recently, Dimitriadis et al. showed that in PEF polymer segments could be located within an amorphous fraction with restricted mobility, different from that in the fully amorphous polymer, leading to possible implications in the mechanical and gas barrier properties.[5] This result was obtained using broadband dielectric spectroscopy on samples prepared by following different protocols that resulted in various degrees of crystallinity. In this same work authors also identified the so-called rigid amorphous fraction (RAF)[19-23] to account for the reduced contributions to the dielectric relaxation and the specific heat capacity

jump at the glass transition temperature (T_g). The RAF is considered as the result of extreme constrains on the amorphous phase when crystallinity is well developed.[19-23]

In this work we report a detailed study on the dielectric relaxation behavior of fully amorphous and cold crystallized PBF, using broadband dielectric spectroscopy. First, we have evaluated the low temperature regime, where we studied the role of glycol length, acid structure and crystallization on the local molecular dynamics, described by the simultaneous presence of two relaxation processes. Then, we have studied the segmental relaxation of this polymer, making special emphasis on how the amorphous phase in the semicrystalline state was affected by the surrounding crystals. In this way, we have interpreted our data using different amorphous fractions, not necessarily phase-separated, that compose the amorphous phase of the semicrystalline material.

2. Experimental section

Poly(butylene 2,5-furanoate) (PBF) was synthesized and characterized as described elsewhere.[11] The PBF chemical structure is presented in Figure 1.

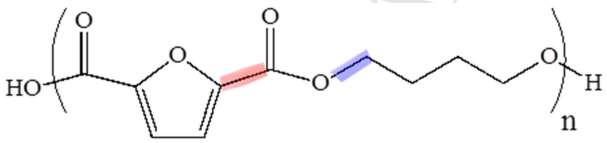

Figure 1. Poly(butylene 2,5-furanoate) (PBF) molecular structure. Red and blue highlighted bonds are those related to the β_2 and β_1 movements respectively, as discussed in section 3.

Broadband Dielectric Spectroscopy (BDS) measurements were carried out in a Novocontrol broadband dielectric spectrometer. This technique allows the study of the complex dielectric permittivity, $\varepsilon^*(\omega) = \varepsilon'(\omega) - i\varepsilon''(\omega)$, where $\varepsilon'(\omega)$ is the dielectric constant and $\varepsilon''(\omega)$ the dielectric losses, as a function of the applied electric field frequency ($\omega = 2\pi f$, f being the frequency) and temperature (T). BDS measurements were performed over a broad frequency window, $10^{-1} \leq f$ (Hz) $\leq 10^7$, using a Novocontrol Alpha S dielectric interface. The temperature was controlled by a nitrogen jet (Quatro from Novocontrol), with a temperature error during every single frequency sweep of ±0.1 K. Samples for dielectric studies were prepared by melt-pressing, allowing to obtain homogeneous films. These samples were pressed between two circular gold electrodes of 40 mm diameter (lower electrode) and 20 mm diameter (upper electrode). In order to avoid any possible short-circuits, Teflon spacers (100 μm thick) were used.

The dielectric studies were conducted as stated in the following lines. The as-prepared PBF film was placed inside the spectrometer cryostat and heated up to 453 K (T_m(PBF) = 437 K [11]), while continuously monitoring its dielectric signal. This final temperature was maintained for 3 minutes and, immediately afterwards, the sample cell

was submerged into a liquid nitrogen reservoir, allowing the sample to reach a temperature of 77 K within a few minutes, and kept at this temperature for 10 min. This procedure permitted to prepare a melt-quenched PBF sample, labeled from now on as **mq-PBF**. For this sample BDS measurements were carried out on heating from 213 K to 393 K. Once the final temperature was reached, the sample cell was again submerged into a liquid nitrogen reservoir and a second heating run was performed, in the range 213 K to 353 K. In this last case, as detailed in section 3 and going in line with recent reports,[11] the PBF it's found in its semi-crystalline state. Then, this sample will be denoted from now on as **sc-PBF**.

In general, BDS data analysis was carried out in terms of the Havriliak-Negami (HN) formalism, where the dielectric function follows the relation:[24]

$$\varepsilon^*(\omega) = \varepsilon_\infty + \sum_x \Delta\varepsilon_x \left[1 + \left(i\omega\tau_{\mathrm{HN}_x}\right)^{b_x}\right]^{-c_x} + \left(\frac{\sigma_{\mathrm{DC}}}{i\varepsilon_0\omega}\right) \quad (1)$$

where $\Delta\varepsilon$ is the dielectric strength of the relaxation and τ_{HN} a characteristic relaxation time; b and c ($0 < b,bc \leq 1$) are shape parameters related to the symmetric and asymmetric broadening, respectively. The summation in equation (1) extends over all the processes present in the experimental window at a specific temperature. Also, the last term in this equation accounts for the contribution of charge carriers to the dielectric signal, where σ_{DC} is the DC conductivity and ε_0 the vacuum permittivity.

From τ_{HN}, the peak relaxation time (τ_{max}) was calculated using the equation:[24-26]

$$\tau_{\mathrm{max}} = \frac{1}{2\pi f_{\mathrm{max}}} = \tau_{\mathrm{HN}} \left[\sin\frac{b\pi}{2+2c}\right]^{-1/b} \left[\sin\frac{bc\pi}{2+2c}\right]^{1/b} \quad (2)$$

where f_{max} is the frequency of maximum loss, and the rest are the HN-function parameters.

Differential Scanning Calorimetry (DSC) measurements were carried out using a TA Instruments Q2000 with a liquid nitrogen cooling system. Temperature-modulated experiments were conducted at a mean rate of 3 K/min, using a 60 s period and ±0.5 K amplitude. Samples for DSC experiments were prepared by encapsulating about 5 mg of PBF in aluminum pans. For the DSC analysis the specific heat increment (Δc_p) associated with the glass transition of the amorphous phase, was calculated from the area under the curve of the heat flow derivative with respect to the temperature, in the region $278 \leq T\ (K) \leq 333$. The glass transition temperature (T_g) was determined from the maximum of the peak. The crystal phase heat of fusion (ΔH_m) was calculated from the difference between the enthalpy associated with the melting endotherm and the cold-crystallization exotherm whenever present.

3. Results

Figure 2 shows the PBF dielectric loss as a function of the applied electric field frequency, for three representative temperatures: 228 K, 323 K and 353 K. Specifically, left column in Figure 1 shows the mq-PBF sample, while the right one the sc-PBF. Also, besides the experimental data points, in Figure 2 we present the total fit and independent contributions from the different relaxation processes.

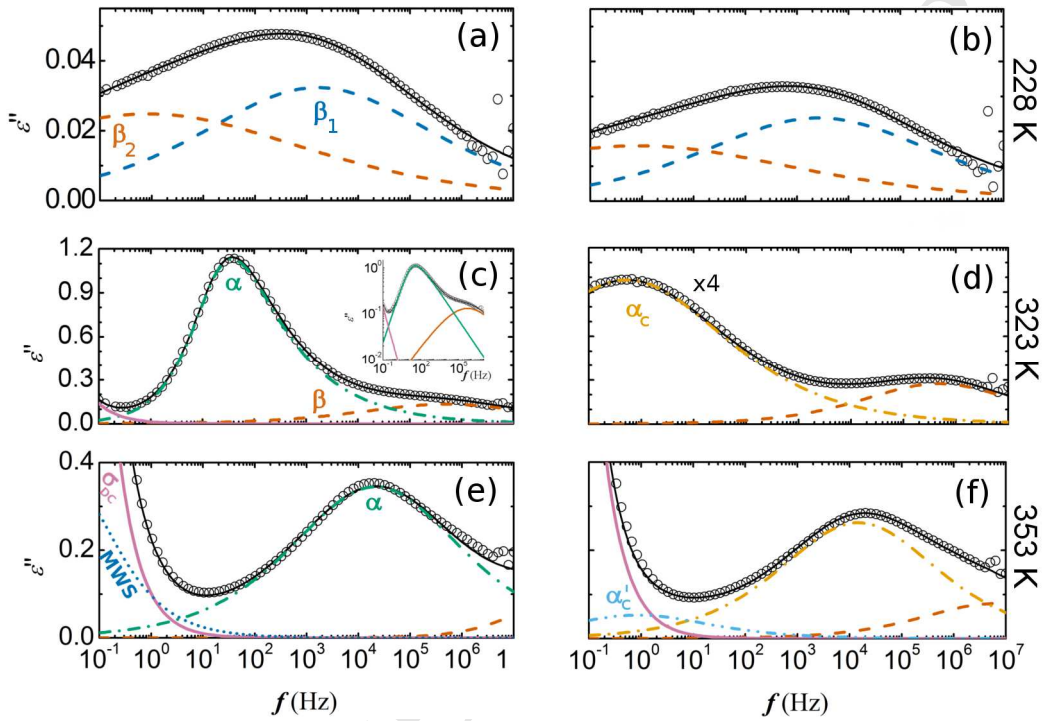

Figure 2. PBF dielectric loss as a function of frequency, for three representative temperatures. Left column represents the mq-PBF sample while right column sc-PBF. Dashed lines refer to the contributions from the different relaxation processes following eq (1); black continuous lines correspond to the total fits. Inset in (c) highlights the power-law tails of the HN relaxation components.

In general, both mq-PBF and sc-PBF samples showed a similar broad distribution of relaxation times at low temperatures (T « PBF glass transition temperature (T_g) = 309 K)[11]. As shown in Figures 2a and 2b, we described this local response by the sum of two Cole-Cole (CC) functions: a specific case of equation (1) where c = 1.[24] We chose this approach considering the strong asymmetry towards low frequencies of the experimental data, not allowing the use of only one dielectric function. Specifically, we labeled the faster peak (*i.e.* the one located at higher frequencies) as β_1 (blue dashed line in Figures 2a and 2b) and the slower one as β_2 (red dashed line in Figures 2a and 2b). The temperature dependence of the CC function parameters is presented in Figure 3. Figure 3a shows the PBF relaxation plot, where in the low temperature regime, these local processes follow an Arrhenius law, described by the equation:[24]

$$\tau_{\max} = \tau_0 \exp\left[\frac{E}{RT}\right] \quad (3)$$

where τ_0 is a time constant, T the temperature, R the gas constant and E the activation energy. Using eq (3) we fitted both local processes (blue and red lines in Figure 3a) and found their activation energies, namely $E_{\beta 1}$ and $E_{\beta 2}$ as reported in Table 1. Figure 3b shows the evolution of the dielectric strength as a function of the temperature. In general, $\Delta\varepsilon$ values were higher in the mq-PBF sample than in the sc-PBF one; however, both cases follow the same trend, being the values almost constant with temperature. Finally, Figure 3c shows that the shape parameter of the CC functions slightly increased with temperature, as expected for local processes.[24]

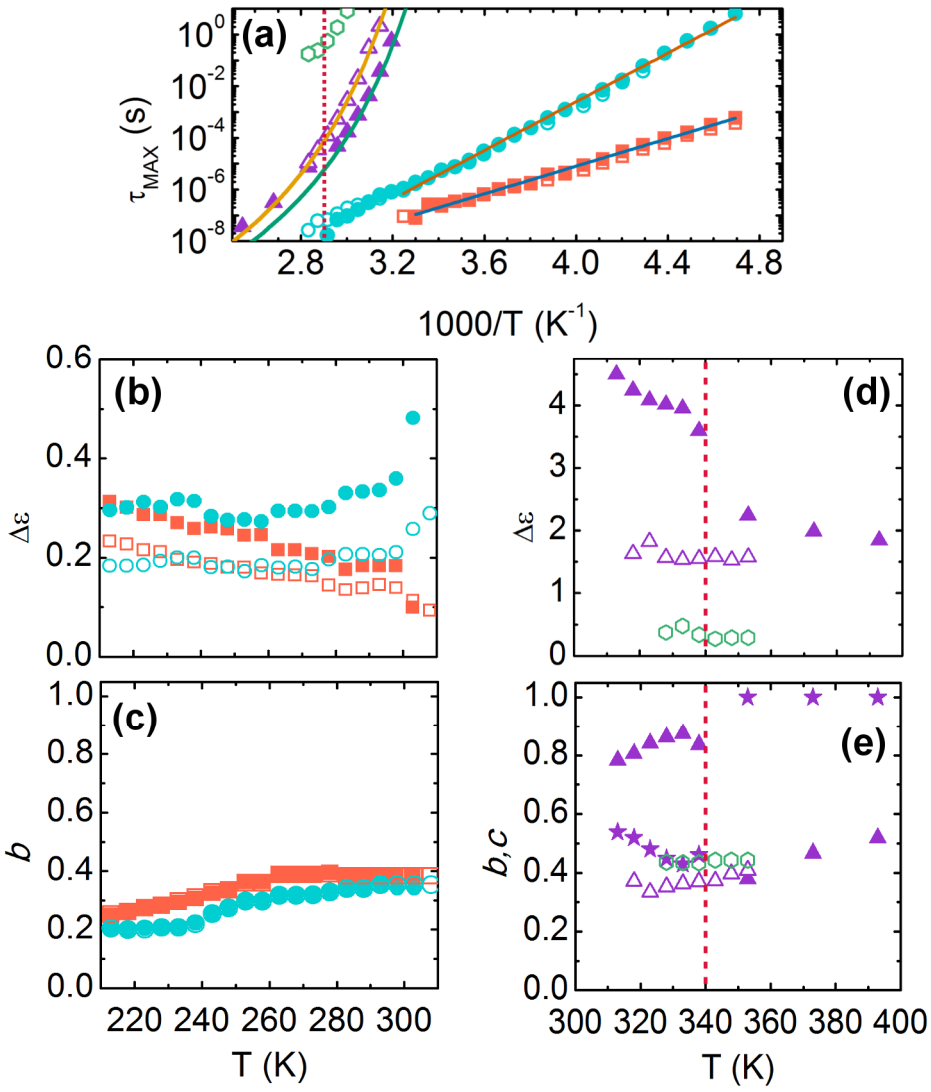

Figure 3. Temperature dependence of dielectric functions parameters of PBF relaxation processes. For all graphs filled symbols refer to mq-PBF and empty symbols to sc-PBF, and specifically: β_1 (red squares), β_2 (blue circles), α (violet triangles), α_c' (green hexagons). (a) Relaxation plot where lines represent fits to the data. (b) Relaxation strength of the local processes. (c) Shape parameters of the local processes. (d) Relaxation strength of the high temperature processes. (e) Shape parameters of the high temperature relaxations. Please notice that in panel (e) the mq-PBF *c*-parameter is represented by stars, while for sc-PBF c = 1, characteristic of a Cole-Cole function, was found. Vertical dotted lines mark the cold-crystallization temperature of PBF.

Table 1. Activation energies (E_A) of PBF, PBT and PBN

Sample	$E_{\beta1}$ (kJ/mol)	$E_{\beta2}$ (kJ/mol)
PBF	50 ± 2	89 ± 1
PBT[27]	43	62
PBN[28]	42	76

As temperature increased and reached values just above the calorimetric T_g, the PBF segmental relaxation (also called α relaxation) appeared as a peak in $\varepsilon''(\omega)$. Figure 2c shows the dielectric loss at 323 K, where the maximum of the mq-PBF α relaxation is located at about 20 Hz, accompanied by the β process in the high frequency side. For the description of this segmental relaxation we used a HN function, eq (1). In Figure 3, we present the temperature dependence of its parameters; specifically, in the PBF relaxation plot (Figure 3a) the α relaxation is depicted by solid triangles. The continuous line passing through them, describes the τ_{max} trend and was fitted following a Vogel-Fulcher-Tammann (VFT) relation:[24]

$$\tau_{\max} = \tau_0 \exp\left[\frac{DT_0}{T - T_0}\right] \quad (4)$$

where τ_0 is a time constant fixed to the value of 10^{-14} s,[29] D a constant related to the fragility of the material and T_0 the Vogel temperature.[24] We highlight that the VFT fitting was performed taken into consideration only the data points below T < 343 K, since from this temperature up cold-crystallization occurs (see below) and the data values lost the lower temperature trend (Figure 3a). The fitting parameters found for this VFT law, as well as the dynamic glass transition temperature of mq-PBF ($T_{g,BDS}$), defined as the temperature at which the segmental relaxation time equates 100 s, are reported in Table 2.

Table 2. VFT parameters for PEF, mq-PBF and sc-PBF

Sample	D	T_0 (K)	$T_{g,BDS}$ (K)
mq-PBF	7.2 ± 0.2	254 ± 1	303 ± 2
sc-PBF	7.4 ± 0.2	260 ± 1	312 ± 2
PEF[5]	7.7 ± 0.2	297 ± 1	359 ± 1

Figure 3d, shows the temperature dependence of the mq-PBF α relaxation dielectric strength (solid triangles). We observed that for temperatures below 343 K, Δε decreases monotonically with temperature, as expected for the segmental relaxation of amorphous polymers;[24] however, at 343 K there is a dramatic Δε drop, being the value, from this point on, almost constant. Also, from this temperature on, the HN function shape parameters changed (Figure 3e). Specifically, the asymmetric broadening of the HN

function (*c*-parameter) suddenly increased to 1, indicating that above 343 K the HN process became a CC function, while the symmetric broadening (*b*-parameter) strongly decreased (broader peak). We associate the observed changes to the cold crystallization of PBF, according to literature reports on polymer crystallization followed by BDS experiments.[30-33] Moreover, the results obtained by us on the sc-PBF sample confirm this interpretation. The empty triangles in the relaxation plot (Figure 3a) represent the sc-PBF τ_{max} values, while the line passing through them is the corresponding VFT fit. This fitting was performed taken into consideration exclusively the empty triangles in the plot; thus, it is coincidental that the mq-PBF values, at T > 343 K, lie just above the found VFT trend. This put into evidence that in the first BDS scan, PBF reached a semicrystalline state at T > 343 K. This result is furthermore confirmed by the sc-PBF Cole-Cole function parameters ($\Delta\varepsilon$ and b), which values are close to the ones observed in mq-PBF at T > 343 K. Finally, from the VFT analysis we found a fragility comparable to that of the amorphous PBF, but an increase of T_0 and $T_{g,BDS}$ in sc-PBF with respect to mq-PBF (Table 2).

The interfaces developed during polymer crystallization might not only affect the polymer segmental dynamics, as the slowing-down shown by the α relaxation (from now on called α_c), but also could give rise to the development of other relaxation processes. In fact, in the mq-PBF sample at T = 353 K, and temperatures above, we had to consider an extra power-law contribution in the low frequency side of the experimental window superimpose on the DC-conductivity contribution (Figure 2e, dotted line). We attribute this relaxation to the charge trapping process occurring at the amorphous-crystalline interfaces, also called Mawell-Wagner-Sillars (MWS) relaxation. Figure 2f shows the sc-PBF sample at the same temperature. Here, the conductivity is lower and the MWS relaxation would lie outside the frequency window; however, a new relaxation process, named α_c', needed to be considered. Going into details, Figure 4 shows that even at the temperatures just above T_g the sc-PBF dielectric loss data, corresponding to the segmental dynamics, depict asymmetry towards low frequencies. Then, as far as we follow the general rule of impeding the HN *c*-parameter values to be greater than 1, in order to properly describe the loss data, we included the new α_c' process in the fitting, being also described by a CC function. The temperature dependence of α_c' is summarized in Figure 3 (open hexagons).

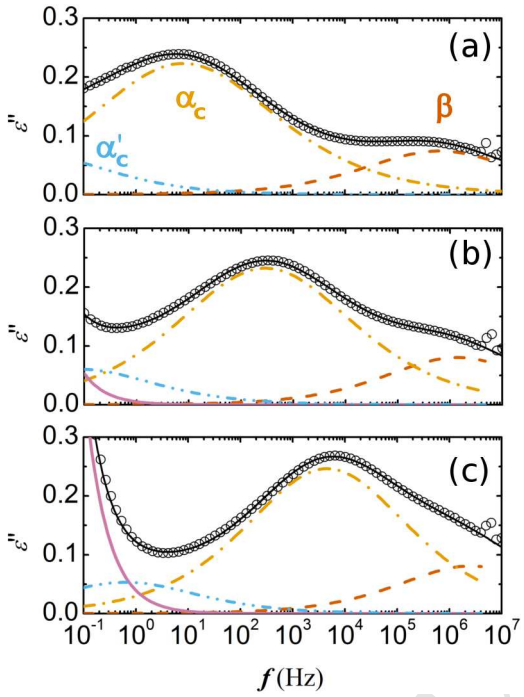

Figure 4. sc-PBF dielectric loss at (a) 328 K, (b) 338 K and (c) 348 K. Dashed lines represent the different fit contributions, solid lines refer to the total relaxation process.

Calorimetric measurements were carried out in order to characterize the thermodynamic state of the PBF samples considered so far. Figure 5a shows the DSC heat flow for mq-PBF (■) and sc-PBF (□). All DSC analysis results are summarized in Table 3, together with the DSC crystalline fraction (χ_c), estimated as $\Delta H_m/\Delta H_m^0$, where the PBF equilibrium melting enthalpy was obtained from the literature (ΔH_m^0 = 129 J/g [34]). We highlight that the crystallinity value obtained for PBF in our present work is much lower than those reported for PEF by Dimitriadis et al. [5]

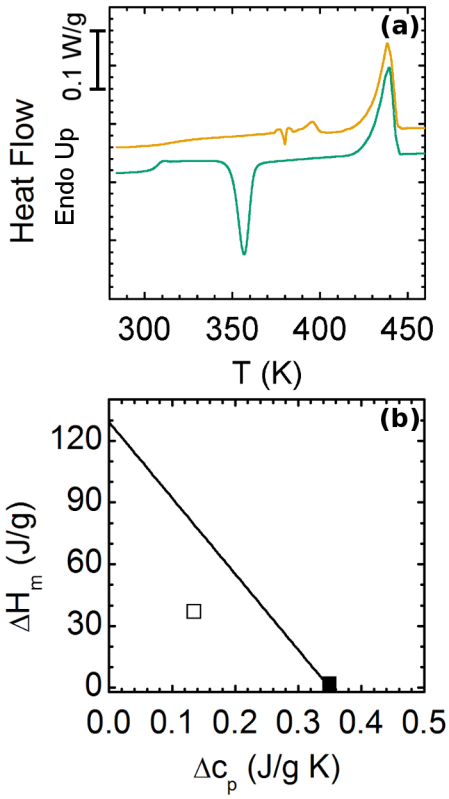

Figure 5. (a) DSC heat flow for mq-PBF (green, ■) and sc-PBF (yellow, □). **(b)** Corresponding plot of the heat of fusion ΔH_m as a function of the specific heat increment at T_g, Δc_p. The solid line was calculated on the basis of a simple two-phase model.

Table 3. DSC analysis results.

Sample	T_g (K)	Δc_p (J/g K)	ΔH_m (J/g)$^{(*)}$	χ_c
mq-PBF (■)	308 ± 1	0.35 ± 0.01	1 ± 1	0.01 ± 0.01
sc-PBF (□)	316 ± 3	0.14 ± 0.03	37 ± 1	0.28± 0.01

*The value corresponds to the difference between the fusion and the cold crystallization enthalpies.

In Figure 5b, we present the heat of fusion (ΔH_m) as a function of the specific heat increment (Δc_p) of the corresponding sample. The solid line in this figure corresponds to the trend expected for a simple two-phase model, *i.e.* where solely the crystalline and amorphous phases are present in the volume of the sample. For this calculation, we have considered the PBF equilibrium melting enthalpy and the specific heat increment of the completely amorphous mq-PBF sample.

4. Discussion

So far, we have presented a broad description of the PBF molecular dynamics using broadband dielectric spectroscopy. Both mq-PBF and sc-PBF showed local relaxations that were analyzed using two CC functions. The simultaneous presence of two β-processes in polymers has been previously observed for several aromatic polyesters, in which the polymer segments present a comparable mobility comparable to that of PBF,

and explained as due to a contribution of different conformationally flexible bonds of the repeating unit;[27,28,33,35-38] while dielectric studies of fully aliphatic polyesters, revealed the presence of a single-mode β process.[30] Considering the chemical structure of PBF (Figure 1) the presence of a two-mode sub-glass relaxation can be ascribed to the different flexibility of the aliphatic glycol subunit and the aromatic acid moiety. Specifically for PBF, β_1 relates to the dielectrically active O−C bond of the ester oxygen to the aliphatic carbon (highlighted in blue in Figure 1), while the low frequency mode β_2 is associated to the C-CA link between the ester group carbon and the aromatic ring (highlighted in red in Figure 1). Taking into account these considerations, the lower value of $E_{\beta 1}$ can be explained considering its relation to the most flexible part of the repeating unit and consequently it is expected to overcome a smaller energy barrier as compared to $E_{\beta 2}$, associated to the less flexible segment (Table 1). It is worth highlighting that in a recent work by Dimitriadis et al[5] on a similar furanoate-based polymer, authors only observed one local relaxation process. In their work, the β process of poly(ethylene-2,5-furanoate) (PEF) has an activation energy of ~58 kJ/mol, value fairly comparable to that of our β_1 process. The presence of just one low temperature process in PEF can be due to the simultaneous presence of a very rigid acid unit and a very short aliphatic segment (just two $–CH_2–$) in the glycolic segment. Both these features make that, at low temperatures, the repeating unit relaxes as one segment. In our case, the detection of two-modes β process can be ascribed to the longer aliphatic subunit (four $–CH_2–$) that makes the glycol segment relaxes at different time values with respect to the furanic acid moiety.

Two-mode sub-glass relaxations have been previously detected by BDS for poly(butylene terephthalate) (PBT),[27] that differs from PBF for the presence of a terephthalic ring instead of a furanic one in the repeating unit, and poly(butylene naphthalate) (PBN)[28], whose repeating unit contains a naphthalene ring. In these works authors showed that, as for PBF, $E_{\beta 1}$ had a lower value than $E_{\beta 2}$ (Table 1); however, quantitatively the PBF local relaxation processes present higher activation energies with respect to those of PBT and PBN, evidencing the higher stiffness of the PBF polymer chains. This effect is particularly evident for the β_2 component associated to C-CA bond between the aromatic ring and the ester group. A possible explanation may be found in the inhibition of the ring flipping in PBF, due to the lower bond angles and the higher polarity of the furanic acid[39] with respect to the terephthalic and naphthalenic ones. So, the hindering of the C-CA bond rotation in PBF could be responsible for the higher $E_A\beta_2$ value.

The PBF local relaxations did not show changes in the dynamics characteristics (relaxation times and relaxation shape) when comparing amorphous and semicrystalline samples; however, we recall that Δε values turned out to be lower for the semicrystalline material (sc-PBF). It is well established[19,40,41] that the more local relaxations in semicrystalline polymers are only affected by crystallinity on the relaxation strength. Moreover, the effect is directly proportional to the crystalline fraction (χ_c). To check this expectation, in figure 6 we show $\varepsilon''/(1-\chi_c)$ as a function of

the frequency at 228 K, for both investigated samples. We observe a good agreement between both set of data points in the high frequency region, *i.e.* for the most local (fast) relaxation processes. However, clear differences are seen in the low frequency part. According to these results, the relaxation components described as β_1 superimpose within uncertainties, whereas those described as β_2 show higher $\Delta\varepsilon$ values for the fully amorphous polymer sample, but with a time-scale and shape quite close in both cases. This result proves that intermolecular interactions have a stronger effect on the molecular motions responsible for β_2, *i.e.* the local relaxation that involves the ring motions, while they do not affect so much the motions involving the aliphatic glycol (β_1 relaxation). This behavior also would explain the different temperature dependences of $\Delta\varepsilon_{\beta_2}$ shown in Figure 3b. These findings can be compared to those reported on PEF,[5] where authors found that semicrystalline samples showed a $\Delta\varepsilon$ decrease (in the single β-process of PEF), in comparison to the fully amorphous material; nonetheless, authors also observed slightly faster relaxation times in samples of higher crystallinity. The whole secondary relaxation of sc-PBF also shows a loss maximum at slightly higher frequencies than in mq-PBF (Figure 6), but the isolated components are not much shifted, indicating that the major effect of crystallinity is the uneven impact in the relaxation strengths of the two β-relaxations.

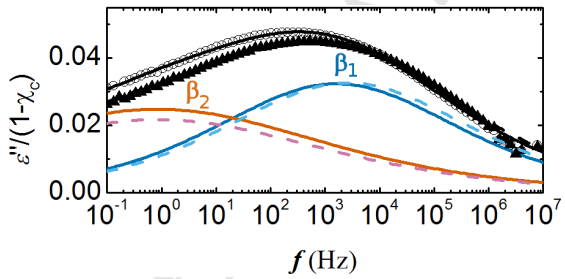

Figure 6. ε''/(1-χ_c) as a function of the frequency, at 228 K, for mq-PBF (○) and sc-PBF(▲).

Considering the segmental relaxation of the totally amorphous mq-PBF sample, if we compare our results with those found for the analogue polymer PEF, we see how changing the glycol length, passing from two methylene groups in PEF to four methylenes in PBF, affects T_0 and consequently $T_{g,BDS}$, but not the D value. In particular, T_0 and $T_{g,BDS}$ decrease by increasing the number of –CH_2–, while the fragility strength parameter D remains almost constant (Table 2). Invariance of D with the number of –CH_2– has been reported in previous studies on aromatic[33,35,42] and aliphatic[30] polyesters.[19,23,43] For example, Sanz et al.,[27,44] demonstrated that the fragility of a polymer mainly depends on the acid subunit and it is independent with respect to the glycol. Specifically, they found a D of 4.9 and 8.1 for poly(butylene terephthalate) PBT and poly(butylene isophthalate) PBI, respectively. Interestingly, the D value obtained for furane-based polyesters turns out to be in between these values, suggesting that the furanic ring confers an intermediate dynamic fragility to the polyester chain with respect to the terephthalic and isophthalic rings.

The amorphous phase of semicrystalline polymers is not unique but depends, to some extent, on the way crystallization is developed.[23,45] This fact is evidenced in our results by the differences found in the dielectric relaxation experiments at 353 K between the sample crystallized on heating from the fully amorphous state (Figure 2e) and that crystallized further up to 393 K (Figure 2f). The segmental relaxation observed for the more crystallized material (sc-PBF), showed changes in relaxation time and shape with respect to the one of the initial fully amorphous mq-PBF crystallized during the first dielectric scan, indicating different dynamical properties. Furthermore, the dielectric strength is reduced more than expected by the dipole blocking in the crystalline phase $\left(\Delta\varepsilon_{\alpha_c}^{\text{sc-PBF}} + \Delta\varepsilon_{\alpha_c'}^{\text{sc-PBF}} \approx 2.0 < (1-\chi_c)\Delta\varepsilon_{\alpha}^{\text{mq-PBF}} \approx 2.8\right)$. In addition, the thermodynamic characteristics of sc-PBF evidence that a simple two-phase model is not adequate to describe this semicrystalline material (Figure 5b). These facts are all in line with previous works in other semicrystalline polymers,[19,21,23,46], as well as with the results found for the analogous polymer PEF.[5] In general, these results have been interpreted in the framework of two major views.

A two-phase approach can be maintained if one considers a framework where the amorphous phase in the semicrystalline material is considered to have different properties (both statically and dynamically) than the fully amorphous polymer. In this view, the main characteristics of the amorphous phase would be the following two: i) lower configurational degrees of freedom than the fully amorphous one (86 % for PBF, determined as: $\Delta c_p^{\text{sc-PBF}} / \left[(1-\chi_c)\Delta c_p^{\text{mq-PBF}}\right]$ = 0.86); ii) dramatically larger dynamic heterogeneities with a distribution of relaxation times more extended towards lower frequencies without a clear limiting value. This second characteristic implies a typical segmental relaxation time, in the semicrystalline polymers, slower than that in the fully amorphous one and a concomitant higher glass transition temperature. However, it should be noted that the extension of the relaxation process towards extremely low frequencies, precludes a trustable determination of the relaxation strength, making unclear if the orientational polarizability remains unaffected in the amorphous phase of semicrystalline polymers or not.

A more conventional approach consists in considering that the amorphous phase of semicrystalline polymers is composed by fractions with different characteristics, not necessarily phase-separated. A primary distinction is made between mobile and rigid amorphous fractions,[19,21,23] where it is considered that Δc_p of the mobile fraction in semicrystalline polymers remains unchanged with respect to that of the fully amorphous phase. Under this approach, one can estimate the mobile amorphous fraction as $\chi_{a,m} = \Delta c_p^{\text{sc-PBF}} / \Delta c_p^{\text{mq-PBF}}$ that, from our DSC results, is equal to 0.59. Then, since $\chi_{a,m} + \chi_c$ = 0.87 for sc-PBF, there would be a rigid amorphous fraction of PBF $\chi_{a,r}$= 0.13. These values are different than those found for PEF[5] ($\chi_{a,m} \approx$ 0.28, $\chi_{a,r} \approx$ 0.35), which could be related with the significantly lower crystallinity of PBF.

Concerning the dynamics of the mobile amorphous fraction, our dielectric spectroscopy analysis approach is based on using two distinct segmental dynamics, which would correspond to two distinguishable mobile amorphous fractions. This arises due to our choice of using Cole-Cole functions in the description of the dielectric loss peak components, avoiding a larger extension of the loss peaks towards low frequencies. Following our approach, if the orientational polarizability of the amorphous phase remains unaffected after crystallization, the whole dielectric relaxation strength of the crystallized sample, defined as $\Delta\varepsilon_{\alpha_c}^{\text{sc-PBF}} + \Delta\varepsilon_{\alpha_c'}^{\text{sc-PBF}}$, should be equal to $\chi_{a,m}\Delta\varepsilon_{\alpha}^{\text{mq-PBF}}$, where $\chi_{a,m}$ is the amorphous fraction in sc-PBF (obtained from DSC analysis) and $\Delta\varepsilon_{\alpha}^{\text{mq-PBF}}$ is the dielectric strength of the fully amorphous sample. Nevertheless, the value obtained, $\Delta\varepsilon_{\alpha_c}^{\text{sc-PBF}} + \Delta\varepsilon_{\alpha_c'}^{\text{sc-PBF}}$ = 2.0, is significantly smaller than the value calculated $\chi_{a,m}\Delta\varepsilon_{\alpha}^{\text{mq-PBF}}$ = 2.4. This difference is beyond uncertainties and consequently implies that, in the assumed approach, a change in the orientational polarizability of the amorphous phase occurs. When comparing these results with those reported for PEF in ref[5] clear differences appear, that can be due to the different approaches used for describing the α-dielectric relaxation of the semicrystalline polymer, namely the shape parameter *c* of the HN function was not restricted to be $c \leq 1$. Using two Cole-Cole components, we obtained a whole dielectric relaxation strength ($\Delta\varepsilon_{\alpha_c}^{\text{sc-PBF}} + \Delta\varepsilon_{\alpha_c'}^{\text{sc-PBF}}$) ~20 % lower than that expected by combining DSC results with the dielectric relaxation strength of the fully amorphous PBF ($\chi_{a,m}\Delta\varepsilon_{\alpha}^{\text{mq-PBF}}$). Contrary, the same calculation with the PEF reported results[5] yields a value of the expected dielectric relaxation strength similar (although slightly lower) to that determined for the fitting of the dielectric data. This could be due to the higher dielectric relaxation strength value resulting from a very low frequency extended tail of the HN loss peak.[19] For instance, using $b = 0.2$ and $c = 3$ in eq. 1, the low frequency tail of the HN function located out of the accessible experimental frequency window accounts for about 20% of the whole dielectric relaxation strength. These somehow contradictory results evidence the important uncertainties in determining the dielectric relaxation strength of the extremely broad segmental relaxation in semicrystalline polymers. The critical role of the different approaches involved in the dielectric analysis precludes a conclusive answer to the question if the polarizability of the amorphous phase becomes affected by polymer crystallization.

Conclusions

We have reported a detailed investigation on the segmental dynamics of amorphous and semicrystalline PBF by means of the combination of DSC and BDS. The obtained results showed some similarities and important differences with respect to a polymer of the same family with a shorter glycol linking between the furan groups. The longer glycol in the PBF plays an important role in the subglass dynamics, leading to a broad

relaxation that must be described using two processes, named β_1 and β_2. These components were related to the more mobile subunit and to the stiffer moiety, respectively. Unexpectedly, the relaxation strength of the slower process β_2 was reduced by crystallization more than expected according to the sample crystallinity, contrary to β_1. On the other hand, our results indicated that the amorphous phase mobility also depends on the glycol subunit length, but the fragility is comparable to PEF, the only furan-based polymer previously investigated by BDS. The PBF cold crystallization led to a slowdown of the segmental dynamics, to a larger extent than for PEF, and a corresponding shift of the glass transition temperature. Cold crystallization also reduces the segmental dielectric relaxation strength, an effect that was characterized as originated by an amorphous phase containing a rigid fraction. The longer glycol subunit reduced the rigid fraction in PBF, as compared to PEF, in line with the lower crystallinity degree.

Acknowledgements

A.A. acknowledges financial support from the Projects MAT2015-63704-P (Spanish-MINECO and EU) and IT-654-13 (Basque Government).

References

[1] Plastics - The Facts 2016: An analysis of European plastics production, demand and waste data, 2016.
[2] S. Kalia and L. Avérous, *Biodegradable and Biobased Polymers for Environmental and Biomedical Applications* (Wiley, 2016).
[3] A. Gandini, T. M. Lacerda, A. J. Carvalho, and E. Trovatti, Chemical reviews **116**, 1637 (2016).
[4] S. K. Burgess, J. E. Leisen, B. E. Kraftschik, C. R. Mubarak, R. M. Kriegel, and W. J. Koros, Macromolecules **47**, 1383 (2014).
[5] T. Dimitriadis, D. N. Bikiaris, G. Z. Papageorgiou, and G. Floudas, Macromolecular Chemistry and Physics **217**, 2056 (2016).
[6] G. Z. Papageorgiou, D. G. Papageorgiou, Z. Terzopoulou, and D. N. Bikiaris, European Polymer Journal **83**, 202 (2016).
[7] S. K. Burgess, O. Karvan, J. R. Johnson, R. M. Kriegel, and W. J. Koros, Polymer **55**, 4748 (2014).
[8] S. K. Burgess, R. M. Kriegel, and W. J. Koros, Macromolecules **48**, 2184 (2015).
[9] S. K. Burgess, D. S. Mikkilineni, D. B. Yu, D. J. Kim, C. R. Mubarak, R. M. Kriegel, and W. J. Koros, Polymer **55**, 6870 (2014).
[10] A. J. J. E. Eerhart, A. P. C. Faaij, and M. K. Patel, Energy & Environmental Science **5**, 6407 (2012).
[11] M. Soccio, M. Costa, N. Lotti, M. Gazzano, V. Siracusa, E. Salatelli, P. Manaresi, and A. Munari, European Polymer Journal **81**, 397 (2016).
[12] M. Gomes, A. Gandini, A. J. D. Silvestre, and B. Reis, Journal of Polymer Science Part A: Polymer Chemistry **49**, 3759 (2011).
[13] J. Ma, X. Yu, J. Xu, and Y. Pang, Polymer **53**, 4145 (2012).
[14] L. Wu, R. Mincheva, Y. Xu, J. M. Raquez, and P. Dubois, Biomacromolecules **13**, 2973 (2012).
[15] J. Zhu, J. Cai, W. Xie, P.-H. Chen, M. Gazzano, M. Scandola, and R. A. Gross, Macromolecules **46**, 796 (2013).
[16] B. Wu, Y. Xu, Z. Bu, L. Wu, B.-G. Li, and P. Dubois, Polymer **55**, 3648 (2014).

[17] J. C. Morales-Huerta, A. Martínez de Ilarduya, and S. Muñoz-Guerra, ACS Sustainable Chemistry & Engineering **4**, 4965 (2016).
[18] M. Y. Zheng, X. L. Zang, G. X. Wang, P. L. Wang, B. Lu, and J. H. Ji, Express Polymer Letters **11**, 611 (2017).
[19] A. Alegria and J. Colmenero, Soft Matter **12**, 7709 (2016).
[20] B. Wunderlich, Progress in Polymer Science **28**, 383 (2003).
[21] A. Esposito, N. Delpouve, V. Causin, A. Dhotel, L. Delbreilh, and E. Dargent, Macromolecules **49**, 4850 (2016).
[22] J. Lee, J. H. Mangalara, and D. S. Simmons, Journal of Polymer Science Part B: Polymer Physics **55**, 907 (2017).
[23] I. Arandia, A. Mugica, M. Zubitur, R. Mincheva, P. Dubois, A. J. Müller, and A. Alegría, Macromolecules **50**, 1569 (2017).
[24] F. Kremer and A. Schönhals, *Broadband Dielectric Spectroscopy* (Springer Berlin Heidelberg, 2003).
[25] S. Havriliak and S. Negami, Journal of Polymer Science Part C: Polymer Symposia **14**, 99 (1966).
[26] S. Havriliak and S. Negami, Polymer **8**, 161 (1967).
[27] A. Sanz, A. Nogales, N. Lotti, A. Munari, and T. A. Ezquerra, Journal of Non-Crystalline Solids **353**, 3989 (2007).
[28] M. Soccio, A. Nogales, M. C. García-Gutierrez, N. Lotti, A. Munari, and T. A. Ezquerra, Macromolecules **41**, 2651 (2008).
[29] C. A. Angell, Polymer **38**, 6261 (1997).
[30] M. Soccio, A. Nogales, N. Lotti, A. Munari, and T. A. Ezquerra, Polymer **48**, 4742 (2007).
[31] A. Sanz, A. Nogales, T. A. Ezquerra, M. Soccio, A. Munari, and N. Lotti, Macromolecules **43**, 671 (2010).
[32] D. E. Martínez-Tong, B. Vanroy, M. Wübbenhorst, A. Nogales, and S. Napolitano, Macromolecules **47**, 2354 (2014).
[33] M. Soccio, A. Nogales, I. Martín-Fabiani, N. Lotti, A. Munari, and T. A. Ezquerra, Polymer **55**, 1552 (2014).
[34] G. Z. Papageorgiou, V. Tsanaktsis, D. G. Papageorgiou, S. Exarhopoulos, M. Papageorgiou, and D. N. Bikiaris, Polymer **55**, 3846 (2014).
[35] M. Soccio, A. Nogales, T. A. Ezquerra, N. Lotti, and A. Munari, Macromolecules **45**, 180 (2012).
[36] A. Nogales, A. Sanz, and T. A. Ezquerra, Journal of Non-Crystalline Solids **352**, 4649 (2006).
[37] S. P. Bravard and R. H. Boyd, Macromolecules **36**, 741 (2003).
[38] A. Alegría, O. Mitxelena, and J. Colmenero, Macromolecules **39**, 2691 (2006).
[39] J. Wu, P. Eduard, S. Thiyagarajan, J. van Haveren, D. S. van Es, C. E. Koning, M. Lutz, and C. Fonseca Guerra, ChemSusChem **4**, 599 (2011).
[40] J. C. Coburn and R. H. Boyd, Macromolecules **19**, 2238 (1986).
[41] M. Soccio, A. Nogales, N. Lotti, A. Munari, and T. A. Ezquerra, Physical review letters **98**, 037801 (2007).
[42] C. Alvarez, I. Šics, A. Nogales, Z. Denchev, S. S. Funari, and T. A. Ezquerra, Polymer **45**, 3953 (2004).
[43] L. Sisti, L. Finelli, N. Lotti, C. Berti, and A. Munari, e-Polymers **3**, 689 (2003).
[44] A. Sanz, A. Nogales, T. A. Ezquerra, N. Lotti, and L. Finelli, Physical Review E **70**, 021502 (2004).
[45] D. E. Martínez-Tong, L. A. Miccio, and A. Alegria, In press (2017).
[46] X. Shen, W. Hu, and T. P. Russell, Macromolecules **49**, 4501 (2016).

Highlights

Molecular dynamics of fully biobased poly(butylene 2,5-furanoate) as revealed by broadband dielectric spectroscopy

Michelina Soccio[a], Daniel E. Martínez-Tong[b,c], Angel Alegría[c,d], Andrea Munari[a], Nadia Lotti[a]

[a]Civil, Chemical, Environmental and Materials Engineering Dept., University of Bologna, Via Terracini 28, 40131, Bologna, Italy
[b]Donostia International Physics Center. P. Manuel Lardizabal 4. 20018, Donostia, Spain.
[c]Centro de Física de Materiales (CSIC-UPV/EHU). P. Manuel Lardizabal 5. 20018, Donostia, Spain.
[d]Departamento de Física de Materiales. Basque Country University (UPV/EHU). Apdo 1072. 20080, Donostia, Spain.

- Local and segmental dynamics of poly(butylene 2,5-furanoate) (PBF) were studied.
- Local dynamics showed a broad relaxation, described by two processes respectively related to the more mobile subunit and to the stiffer moiety.
- Amorphous phase mobility depended on the glycol subunit length, while the fragility was mainly correlated to the acid moiety.
- Cold crystallization led to a slowdown of the segmental dynamics and concomitant reduced dielectric relaxation strength.
- The amorphous phase of semicrystalline PBF was described using different fractions, including a completely rigid fraction.